σ-Aromaticity

International Edition: DOI: 10.1002/anie.201410737
German Edition: DOI: 10.1002/ange.201410737

# The σ-Aromatic Clusters $[Zn_3]^+$ and $[Zn_2Cu]$: Embryonic Brass**

*Kerstin Freitag, Christian Gemel, Paul Jerabek, Iris M. Oppel, Rüdiger W. Seidel, Gernot Frenking,* Hung Banh, Katharina Dilchert, and Roland A. Fischer**

*Dedicated to Professor Manfred Scheer on the occasion of his 60th birthday*

***Abstract:*** *The triangular clusters $[Zn_3Cp^*_3]^+$ and $[Zn_2CuCp^*_3]$ were obtained by addition of the in situ generated, electrophilic, and isolobal species $[ZnCp^*]^+$ and $[CuCp^*]$ to Carmona's compound, $[Cp^*Zn{-}ZnCp^*]$, without splitting the Zn–Zn bond. The choice of non-coordinating fluoroaromatic solvents was crucial. The bonding situations of the all-hydrocarbon-ligand-protected clusters were investigated by quantum chemical calculations revealing a high degree of σ-aromaticity similar to the triatomic hydrogen ion $[H_3]^+$. The new species serve as molecular building units of $Cu_nZn_m$ nanobrass clusters as indicated by LIFDI mass spectrometry.*

The triatomic hydrogen (trihydrogen) ion $[H_3]^+$ is one of the most abundantly generated ions in the universe. It is highly reactive and is believed to play an important role in the interstellar formation of more complex molecules.[1] The regular triangular structure is held together by only two electrons providing the most simple and fundamental example for a delocalized three-center–two-electron (3c2e) bond (Figure 1).[2] Calculations of ring-current density maps suggest the $[H_3]^+$ ion is prototypical for σ-aromatic molecules. The situation becomes more complicated in the heavier homologue $[Li_3]^+$.[3] The global minimum structure of this metallacycle is also a regular triangle with considerable resonance stabilization energy, however, ring-current density calculations do not support σ-aromaticity.[4] Recently, the ligand-protected triangular gold cluster $[(LAu)_3]^+$ (L = 1,3-bis(2,6-diisopropylphenyl)imidazol-2-ylidene) was isolated.[5] This $[Au_3]^+$ system is isolobal to $[H_3]^+$ $LAu^+ \leftrightarrow H^+$. Only 6s orbitals contribute to the delocalized 3c2e $Au_3$ bonding of the core. Another close analogue is the homoleptic $[Hg_3]^+$ cluster cation of $[Hg_3(\mu\text{-dmpm})_4][O_3SCF_3]_4$.[6] The mixed-ligand $Pd_3$ cluster $[Pd_3(\mu\text{-SPh})_3(PPh_3)]^+$ was the first d-block analogue of the π- aromatic cyclopropenyl cation $[C_3H_3]^+$ (Figure 1).[7]

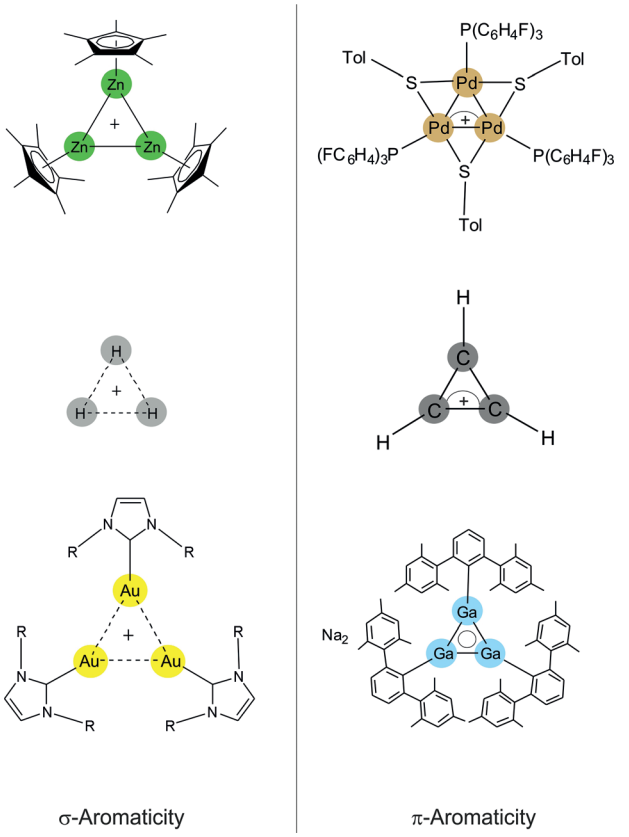


***Figure 1.*** Reference examples for σ- and π-aromatic triangular molecules. Top left: $[Zn_3Cp^*_3]^+$ (this work); top right: $[\{(STol)(PAr_3)Pd\}_3]^+$ (Ar = $C_6H_4F$)[7] bottom left: $[(LAu)_3]^+$;[5] bottom right: $[\{MesC_6H_3)Ga\}_3]^{2-}$ (Mes = 2,4,6-$Me_3C_6H_2$).[8] Middle: the corresponding fundamental structure.

Isolable, ligand-protected $M_3$ main-group metal clusters have been in the focus of research since the 1980s and one particular highlight was the $Ga_3$ cluster $Na_2[(Mes_2C_6H_3)Ga]_3$ (Mes = 2,4,6-$Me_3C_6H_2$) reported by Robinson et al in 1995.[8] From a synthetic point of view it is quite suggestive to regard the trigonal, ligand-stabilized (metallo-aromatic) clusters $[M_3]L_n$ as the embryonic state of metal (nano) clusters. All larger clusters and bulk metals feature triangular close packed

[*] Dr. K. Freitag, Dr. C. Gemel, Dr. R. W. Seidel, H. Banh, K. Dilchert, Prof. Dr. R. A. Fischer
Inorganic Chemistry II—Organometallics and Materials
Faculty of Chemistry and Biochemistry, Ruhr University Bochum
44780 Bochum (Germany)
E-mail: roland.fischer@rub.de
Dr. P. Jerabek, Prof. Dr. G. Frenking
Department of Chemistry
Philipps University Marburg
35032 Marburg (Germany)
E-mail: frenking@chemie.uni-marburg.de
Prof. Dr. I. M. Oppel
Institut of Inorganic Chemistry
RWTH Aachen University, 52056 Aachen (Germany)

[**] This work was funded by the Deutsche Forschungsgemeinschaft (individual grant Fi-502/23-2) and by RESOLV (EXC 1069). The dissertation project of K.F. was supported by the German Chemical Industry Fund (https://vci.de/fonds) and the Ruhr University Research School (http://www.research-school.rub.de/). H.B. is grateful for a scholarship of the German Chemical Industry Fund.

Supporting information for this article is available on the WWW under http://dx.doi.org/10.1002/anie.201410737.

and tightly bonded $\mathbf{M_3}$ units. Thus, it may be anticipated that $[\mathbf{M_3}]L_n$ species may be useful as building blocks for larger clusters in a bottom-up approach. However, very bulky and strongly binding (non-fluxional) ligands L, such as $Mes_2C_6H_3$, are not likely to favor cluster growth. In our contribution we report on the new $\mathbf{M_3}$ species $[Zn_3Cp^*_3]^+$, abbreviated as $[\mathbf{Zn_3}]^+$ ($Cp^* = \eta\text{-}C_5Me_5$) and as well we present its neutral Cu/Zn substituted analogue $[Zn_2CuCp^*_3] = [\mathbf{Zn_2Cu}]$. These two σ-(metallo)aromatic systems serve as embryonic models for both, zinc and brass, respectively, $[\mathbf{Zn_2Cu}]$ being the classic text-book example of a Hume–Rothery intermetallic phase.[9] Previously, we have demonstrated the conceptual relationship between one-electron ZnR ligands and the hydrogen radical with respect to coordination to transition-metal centers. For instance, Carmona's $Zn^I$ dimer $[Zn_2Cp^*_2]$, which is isolobal to $H_2$, that is, Cp*Zn↔H, indeed adds to unsaturated transition-metal fragments $[L_nM]$ across the Zn–Zn bond to yield $[L_nM(ZnCp^*)_2]$, similar to the oxidative addition of $H_2$ to metal complexes forming dihydrides $[L_nM(H)_2]$.[10] In this context it is quite instructive to recognize the icosahedral, quasi-homoleptic $[Mo(ZnMe)_9(ZnCp^*)_3]$ as being stable and readily accessible metallo-analogue of the low-temperature, matrix-isolated polyhydride complex $[WH_{12}]$.[11,12] Interestingly, the formula $[WH_{12}]$ should better be written as $[WH_6(H_2)_4]$. Six hydride ligands and for side-on "Kubas-type"[13] dihydrogen ligands are coordinated to the W center. In contrast, the core structure $[\mathbf{WZn_{12}}]$ features twelve identical W–Zn interactions and no indication for "side-on" bonded $Zn_2$ units. For the reasons outlined above, we became interested in identifying synthetic pathways to yield the homometallic and homoleptic all-hydrocarbon-ligand-protected triangular cluster $[Zn_3Cp^*_3]^+$ and investigate the bonding situation in relation to the $[H_3]^+$ ion. In addition we aimed to find an example for a side-on bonded σ(Zn–Zn) moiety, resulting in a dihydrogen analogous metal complex $[L_nM\{\eta^2\text{-}(Cp^*Zn\text{-}ZnCp^*)\}]$.

The low-temperature reactions of equimolar amounts of $[Zn_2Cp^*_2]$ with the in situ generated coordinatively unsaturated (however solvated) species CuCp* and $[ZnCp^*]^+$ (see Experimental Section) leads to the formation of the salt $[Zn_3Cp^*_3][BAr^F_4]$ (**1**) and the neutral compound $[Zn_2CuCp^*_3]$ (**2**) (Figure 2, top). Both compounds are obtained as crystalline solids after standard workup and very careful low-temperature crystallization procedures. Elemental analyses of **1** and **2** (C, H, Zn, and Cu) are in reasonable agreement with the proposed molecular formulas. The calculated data and measured analytical values deviate from each other somewhat more than usual for (reactive) organometallic compounds. This discrepancy is explained by the high thermal instability as well as high sensitivity to air and moisture of **1** and **2**. Both compounds are very labile and rapidly decompose at room temperature, in solution as well as in the solid state. Notably, crystalline **1** cannot be re-dissolved without decomposition. For example, a yellow solution of **1** in $CD_2Cl_2$ becomes colorless within a few seconds. However, a singlet at $\delta =$ 2.14 ppm is detected in by $^1$H NMR spectroscopy which can be assigned to **1**, in addition to signals for $[Zn_2Cp^*_2]$, $[ZnCp^*_2]$, and $BAr^F_3$. This observation points to a decomposition mechanism with aryl group ($Ar^F$) migration from the

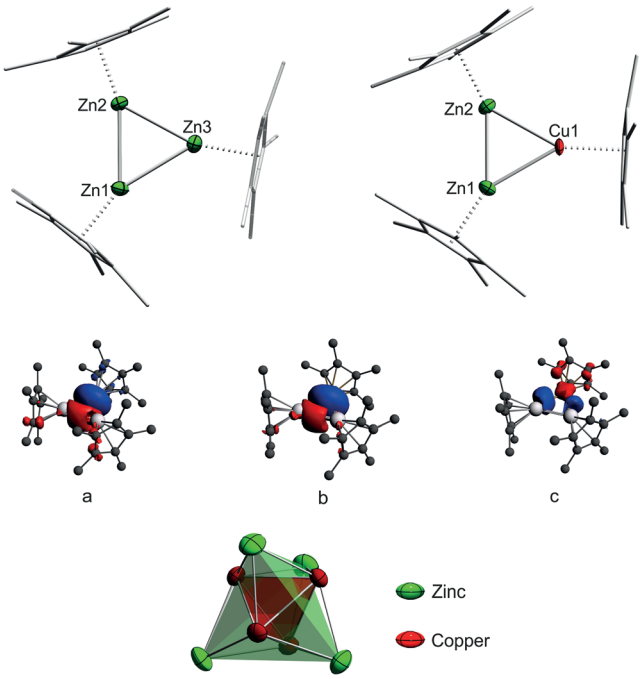


***Figure 2.*** Top: Crystal structures of $[\mathbf{Zn_3}]^+$ (left) and $[\mathbf{Zn_2Cu}]$ (right) from **1** and **2**. Thermal ellipsoids of the metal atoms are set at 50% probability. Hydrogen atoms are omitted for clarity. For bond lengths and angles see Experimental Section. Middle: Deformation densities $\delta\rho$ which are associated with the pair-wise orbital interactions in $[Zn_3Cp^*_3]^+$ and in $[Zn_2Cp^*_2CuCp^*]$. a) $[Zn_2Cp^*_2]\rightarrow[ZnCp^*]^+$ σ donation. b) $[Zn_2Cp^*_2]\rightarrow[CuCp^*]$ σ donation. c) $[Zn_2Cp^*_2]\leftarrow[CuCp^*]$ π back-donation. The direction of the charge flow is from red to blue. Bottom: Tetrahedral star core structure $[Cu_4Zn_4]$ in the ligand-protected cluster $[(CuCN\mathit{t}Bu)_4(ZnCp^*)_4]$. The $[Cu_4Zn_4]$ structure features the triangles $ZnCu_2$ and $Cu_3$.

$[BAr^F_4]^-$ ion to the electrophilic $[Zn_3Cp^*_3]^+$ ion (see Supporting Information, Figure S6), possibly leading to formation of $ZnAr^F$ species (not identified, so far). Calculated from the signal integrals, approximately 60% of the sample spontaneously converts during the dissolution process (also at lower temperatures $\ll 0$ °C). The rate of further decomposition of $[\mathbf{Zn_3}]^+$ is rather slow once the compound is completely dissolved. This effect is quite interesting and important, however not fully understood. It can be speculated that the solvation mechanism and peculiar solvent stabilization effects of the anion and/or the cation may be involved (solvent/crystal-surface interactions during dissolution). In contrast, the less-electrophilic, neutral cluster $[CuZn_2]$ (**2**) can be dissolved without decomposition in a variety of organic solvents. The $^1$H NMR spectrum of **2** recorded in $C_6D_6$ solution at 25 °C reveals two singlets with an integral ratio of 1:2. The $^{13}$C NMR spectrum features the expected four signals. Liquid-injection field desorption ionization mass spectrometry (LIFDI-MS) does not show the molecular ion peak for $[Zn_2CuCp^*_3]^+$. Instead, the higher nuclear species $[Zn_4Cu_3Cp^*_5]^+$ ($m/z$ 1128), $[Zn_4Cu_2Cp^*_6]^+$ ($m/z$ 927), as well $[Zn_3CuCp^*_3]^+$ ($m/z$ 660) are clearly identified. This observation suggests a rich chemistry of Zn/Cu cluster growth can take place in solution, if the right precursors and conditions can be identified. Recently we reported the synthesis of the

  

ligand protected $M_8$ cluster $[(CuCNtBu)_4(ZnCp^*)_4]$ which features a $Cu_4Zn_4$ tetrahedral star core showing nested $Cu_4$ tetrahedra inside a capping $Zn_4$ shell (Figure 2, bottom).[14] The structure of the metal core of this cluster is based on interconnected triangles $Cu_3$ and $ZnCu_2$. Thus, $[\mathbf{Zn_3}]^+$ as well as $[\mathbf{Zn_2Cu}]$ can well be regarded as building units of such larger intermetallic clusters with more complex structures. The structure of the observed fragment $[Zn_4Cu_3Cp^*_5]^+$ may be related to this $Cu_4Zn_4$ cluster (Figure 2, bottom).

We emphasize that $[Zn_2Cp^*_2]$ and $[ZnCp^*]$ itself can be regarded as the primitive building blocks or synthetic equivalents of "atomic Zn" for systematic zinc-cluster growth. In fact, treatment of $[Zn_2Cp^*_2]$ with $[Fc][BAr^F_4]$ (Fc = ferrocinium) in the presence of $ZnMe_2$ yields $[Zn_{10}Cp^*_6(CH_3)][BAr^F_4]$ (see Supporting Information). It is the first example of ligand-protected higher nuclearity Zn clusters $[Zn_n]L_m$ ($n,m > 3$). Details on the synthesis, structure, and bonding situation of this $Zn_{10}$-cluster will be given elsewhere.

The solvated compound $\mathbf{1}\cdot 0.5\,C_6H_5F$ crystallizes in the monoclinic space group $P2_1/c$ with two distinct formula units in the asymmetric unit. Figure 2 (top) shows a plot of only one crystallographic distinct cation of **1** for clarity (see Experimental and Supporting Information). The solvate-free compound **2** crystallizes in the triclinic space group $P\bar{1}$. Both core structures $[Zn_3]^+$ and $[Zn_2Cu]$ reveal nearly perfect equilateral triangle arrangements of the metal atoms M with bond angles of 61.06(2)°, 59.22(1)° and 59.71(2)° for **1** and 60.34(3)°, 59.33(2)°, and 60.34(3)° for **2**. The Zn–Zn bond lengths of **1** are almost identical with an average of 2.430(1) Å. In contrast **2** has two equal Zn–Cu bonds of 2.381(1) Å and a slightly shortened Zn1–Zn2 bond (2.357(1) Å). All M–M (M = Cu, Zn) distances are elongated by 5.5% (**1**) and 2.3–3.3% (**2**) as compared with $[Zn_2Cp^*_2]$ (2.305(3) Å).[15] The above mentioned $Cu_4Zn_4$ cluster $[(CuCNtBu)_4(ZnCp^*)_4]$ has a Cu–Zn distance of 2.498(2) Å (stretched by 5% as compared to **2**).[14] The average Zn–$Cp^*_{centroid}$ distance (1.85 Å) of **1** is distinctly shorter than in $[Zn_2Cp^*_2]$ and in $[(CuCNtBu)_4(ZnCp^*)_4]$ (2.055 Å) and matches well with other cationic dizinc species as a result of the enhanced ionic interaction.[16] The M–$Cp^*_{centroid}$ distances of **2** (both 1.88 Å) are shortened compared to that found in $[Zn_2Cp^*_2]$ (2.04 Å);[15] nevertheless they are in good agreement with average values of Zn–$Cp^*_{centroid}$ (1.83–2.19 Å) and Cu–$Cp^*_{centroid}$ (1.82–1.96 Å) distances found in reference compounds. Thus, the much more reactive, electrophilic nature of the $[\mathbf{Zn_3}]^+$ unit with respect to $[\mathbf{Zn_2Cu}]$ is nicely indicated by the structural parameters.

To get a more detailed insight into the bonding situations of the title clusters, we calculated the structures of the cation $[Zn_3Cp^*_3]^+$ and the isoelectronic neutral homologue $[Zn_2CuCp^*_3]$ for isolated molecules using the *meta*-GGA functional M06L which intrinsically considers dispersion interactions[17] in conjunction with TZVPP basis sets[18] and we analyzed the nature of the bonding with an energy decomposition analysis (EDA). Details of the theoretical methods are given in the Supporting Information. The calculated structural parameters of **1** are in good agreement with the experimental data. The calculations give nearly identical Zn–Zn distances for the $[\mathbf{Zn_3}]^+$ core which are only a bit longer than the experimental data from single-crystal X-ray diffraction analysis. However the crystal structure shows a slightly distorted zinc triangle which can be due to intermolecular interactions between the various species packed together in the unit cell of the crystal. Interestingly, significantly larger deviations are found between the calculated and experimental bond lengths of **2**. The calculations suggest that the Zn–Zn bond in $[Zn_2Cu]$ is clearly longer (2.531 Å) than in $[\mathbf{Zn_3}]^+$ (2.464/2.465 Å) and also much longer than in $[Zn_2Cp^*_2]$ (as the reference for $\sigma_{Zn-Zn}$) interactions: 2.305(3) Å). Accordingly, the calculated Zn–Cu bonds of 2.355/2.359 Å are shorter than the Zn–Zn bonds. However, the analysis of the X-ray data leads to almost equal bond lengths Zn–Zn 2.357 Å and Zn–Cu 2.381 Å. While the value for Zn–Cu is in reasonable agreement with the calculated data for the Zn–Cu bond, the Zn–Zn value is much shorter than the theoretical value for the Zn–Zn bond. Therefore, we optimized the structure of **2** using the GGA functional BP86[19] in conjunction with the D3 method for dispersion forces by Grimme et al.[20] at the BP86(D3)/TZVPP level. The calculations gave similar values to the M06L/TZVPP results (Supporting Information). From Pyykkö's and Atsumis table for molecular single-bond covalent radii for the elements it follows that that unperturbated $\sigma_{Zn-Zn}$ bonds should be a bit longer (2.36 Å) than the respective $\sigma_{Cu-Zn}$ bonds (2.30 Å).[21] The absolute values in a three-membered ring can be expected to deviate from average values, but the order $d$(Zn–Zn) > $d$(Cu–Zn) should be the same. We optimized the geometry of **2** with several other functionals and different basis sets and with ab initio methods using MP2. While the absolute values for the Zn–Zn and Zn–Cu distances varied to some degree, the trend was always $d$(Zn–Zn) > $d$(Zn–Cu).[22] Finally, we optimized the geometry of **2** at the BP86(D3)/TZVPP level where we kept the bond length Zn–Zn frozen at the experimental value of 2.357 Å. The calculation gave Zn–Cu distances of 2.327/2.323 Å which are still shorter than the Zn–Zn bond. It is noteworthy that the structure with the frozen bond is only 0.7 kcal mol$^{-1}$ higher in energy than the fully optimized molecule. Based on the above computational data and reasoning, it is valid to suggest that the significantly elongated Zn1–Zn2 bond of 2.531 Å found for the calculated structure $[Zn_2Cu\ Cp^*_3]$ is nicely indicative for a "side-on" bonded $\sigma_{Zn-Zn}$ unit donating electron density to the electron-deficient [CuCp*] fragment and cluster **2** may thus be also written as a complex of formula: $[Cp^*Cu(\eta^2\text{-}Cp^*Zn\text{-}ZnCp^*)]$.

We analyzed the nature of the metal–metal bonding in the triangular clusters with the EDA-NOCV method (NOCV = natural orbitals for chemical valence)[18] Table 1 shows the numerical results for the interactions between the fragments $[ZnCp^*]^+$ and $[Zn_2Cp^*_2]$ in the $[Zn_3Cp^*_3]^+$ ion. The intrinsic bonding interaction of $\Delta E_{int} = -83.2$ kcal mol$^{-1}$ is quite strong. The major component of the total orbital interactions $\Delta E_{orb} = -59.1$ kcal mol$^{-1}$ comes from the σ donation $[Zn_2Cp^*_2] \rightarrow [ZnCp^*]^+$ into the formally empty 4 s valence orbital of Zn at the [ZnCp*] fragment. This situation becomes clear from the shape of the associated deformation density $\delta\rho$ which is shown in Figure 2 (Middle).

  

***Table 1:*** EDA-NOCV results for the cation $[Zn_3Cp^*_3]^+$ and for $[Zn_2CuCp^*_3]$ at BP86/TZ2P + //M06L/TZVPP.[a]

| Energy | $[Zn_3Cp^*_3]^+$ | $[Zn_2CuCp^*_3]$ |
|---|---|---|
| $\Delta E_{int}$ | −83.2 | −54.9 |
| $\Delta E_{Pauli}$ | 81.6 | 99.6 |
| $\Delta E_{elstat}$ | −74.0 (44.9%) | −105.4 (68.3%) |
| $\Delta E_{orb}$ | −90.8 (55.1%) | −49.0 (31.8%) |
| $\Delta E_{orb,\sigma}$ | −59.1 (65.1%) | −21.8 (44.5%) |
| $\Delta E_{orb,\pi\parallel}$ | −7.9 (8.7%) | −16.5 (33.7%) |
| $\Delta E_{orb,\pi\perp}$ | −3.2 (3.5%) | −2.7 (5.5%) |
| $\Delta E_{orb,rest}$ | −20.6 (22.7%) | −15.4 (31.3%) |

[a] The interacting fragments are $[ZnCp^*]^+$ and $[Zn_2Cp^*_2]$ for $[Zn_3Cp^*_3]^+$ and $[CuCp^*]$ and $[Zn_2Cp^*_2]$ for $[Zn_2CuCp^*_3]$. The energy values are given in kcal mol$^{-1}$.

A slightly different situation is found for the interaction between $[CuCp^*]$ and $[Zn_2Cp^*_2]$ in $[Zn_2CuCp^*_3]$ (**2**). Table 1 shows that the intrinsic interactions $\Delta E_{int} = -54.9$ kcal mol$^{-1}$ in **2** are a bit weaker than in $[Zn_3Cp^*_3]^+$ which may be explained by the neutral fragment $[CuCp^*]$ being a weaker acceptor than the isolobal, however cationic, $[ZnCp^*]^+$. This situation also explains why there are two dominant orbital interactions in **2**. Table 1 shows that the σ-donation $[Zn_2Cp^*_2]\rightarrow[CuCp^*]$ (−21.8 kcal mol$^{-1}$) is only slightly stronger than the π back-donation $[Zn_2Cp^*_2]\leftarrow[CuCp^*]$ (−16.5 kcal mol$^{-1}$). Figure 2b,c (Middle) show the associated charge flow of these orbital interactions. Thus, the description of **2** as "side-on" coordinated dizinc complex at the electron-deficient fragment $d^{10}$-$LCu^I$ (L = Cp*) is justified. The metal–metal bonding situation in the triangular cores $[\mathbf{Zn_3}]^+$ and $[\mathbf{Zn_2Cu}]$ which have just two cluster valence electrons (cve) for in-plane bonding is interesting in view of the controversial discussion about σ aromaticity in cyclic $[Li_3]^+$.[3,4,23] The bonding in $[Li_3]^+$ may be compared with metal–metal bonding in **1** and **2** when the effect of the filled d-shell and the M–Cp* bonding is neglected. We calculated the nucleus-independent chemical shift (NICS) values of $[Zn_3Cp^*_3]^+$ (**1**) and $[Zn_2CuCp^*_3]$ (**2**) at the center of the rings at M06L/TZVPP and found strongly negative NICS(0) of −38.0 ppm for **1** and −42.3 ppm for **2** which are even more negative than the reported value for $[Li_3]^+$ (−11.2 ppm).[4,23] A detailed analysis of the metal–metal bonding in **1** and **2** will be the subject of a subsequent theoretical study. At this point we would like to note that hypothetical molecular cluster species, such as $[ZnCu_2Cp^*_3]$ (cve = 1) or $[Cu_3Cp^*_3]$ (cve = 0), are very unlikely to exist, because of a lack of cluster valence electrons: However a mixed-ligand species $[ZnCu_2](X_2L)$, with X = Cp* or other electron-withdrawing "anionic" substituents, and L being a neutral donor ligand, would match the required cve = 2. This control of cve by a mixed-ligand protecting shell is demonstrated for the Cu/Zn system by the cluster $[(CuCN\mathit{t}Bu)_4(ZnCp^*)_4]$ which features cve = 8.[12]

In summary, we found that **1** and **2** can nicely be compared to the dihydrogen complexes $[L_nM(\eta^2\text{-}H_2)]$, in which $H_2$ side-on coordinates to transition-metal centers that are coordinatively unsaturated. The extensive studies of such kinds of complexes showed that crucial factors for their stabilization are positively charged metal centers, less-electron-rich metals, especially first- and second-row metals, and a good balance of σ donation and π back-donation.[18] Our results demonstrate that these factors can be transferred to "side-on" coordinated $[Zn_2Cp^*_2]$, as for compounds **1** and **2** at least two criteria are fulfilled. Further investigations on the "side-on" binding mode of $[Zn_2Cp^*_2]$ at transition-metal centers are part of our research and will be reported elsewhere, soon. The appealing analogy between $[H_3]^+$ and both, $[\mathbf{Zn_3}]^+$ and $[\mathbf{Zn_2Cu}]$ is of heuristic value to guide our continuing efforts of developing a tool box for bottom-up synthesis of Hume–Rothery inspired molecular intermetallics.

## *Experimental Section*

All manipulations were carried out using standard Schlenk and glovebox techniques as well as dry argon. All used solvents were degassed, dried, and saturated with Ar prior to use. $[Zn_2Cp^*_2]$, $[ZnCp^*_2]$, $[LiCp^*]$, and $[H(Et_2O)_2][BAr^F_4]$ were prepared according to literature procedures (References are given in the Supporting Information).

**1**: $[Zn_2Cp^*_2]$ (100 mg, 0.249 mmol), $[ZnCp^*_2]$ (84 mg, 0.249 mmol), and $[H(Et_2O)_2][BAr^F_4]$ (252 mg, 0.249 mmol) were dissolved in fluorobenzene (3 mL). The solution was stirred for 1 h at 20 °C. After evaporation of the solvent, the oily residue was washed twice with *n*-hexane (2 mL) and the yellow powder (quantitative yield) was dried in the vacuum. Needle-shaped yellow crystals of **1**·0.5 $C_6H_5F$ where formed by slow diffusion of *n*-hexane into a saturated fluorobenzene solution at −30 °C. Yield: 289 mg (0.249 mmol). Elemental analysis (%) calcd for $Zn_3C_{65}H_{59.5}BF_{24.5}$: C 51.72, H 3.98, Zn 12.72; found: C 49.47, H 3.93, Zn 11.03. IR: $\tilde{\nu}$ = 2900, 1596, 1443, 1401, 1375, 1342, 1264, 1108, 997, 925, 879, 831, 738, 706, 675, 663, 578, 500, 443 cm$^{-1}$.

**2**: CuCl (50 mg, 0.498 mmol) in THF (2 mL) was added to a suspension of LiCp* (71 mg, 0.498 mmol) in THF (3 mL) at −78 °C. To this reaction mixture $[Zn_2Cp^*_2]$ (200 mg, 0.498 mmol) in THF (3 mL) was added at −78 °C. $[Zn_2Cp^*_2CuCp^*]$ precipitated as a pale yellow, microcrystalline solid. The supernatant THF solution was removed by cannula and the solid re-dissolved in toluene (8 mL) at −78 °C. Yellow crystals, suitable for single-crystal X-ray diffraction (yields about 35%) were obtained after storage of this solution at −30 °C. The crystals were isolated, washed three times with *n*-hexane (3 mL) at −30 °C, and blow-dried: $^1$H NMR ($C_6D_6$, 25 °C): $\delta$ = 2.07 (s, 30H, $ZnC_5Me_5$), 2.23 ppm (s,15H, $CuC_5Me_5$); $^{13}$C NMR ($C_6D_6$, 25 °C): $\delta$ = 10.91 (s, $ZnC_5\mathit{Me}_5$), 12.18 (s, $CuC_5\mathit{Me}_5$),104.65 (s, $CuC_5Me_5$), 110.35 ppm ($ZnC_5Me_5$). Elemental analysis (%) calcd for $CuZn_2C_{30}H_{45}$: C 60.05, H 7.55, Cu 10.59, Zn 21.79; found: C 58.68, H 7.36, Cu 11.22, Zn 21.96. LIFDI-MS: *m*/*z* 1128 ($[Zn_4Cu_3Cp^*_5]^+$), 927 ($[Zn_2Cp^*_2CuCuZn_2Cp^*_2]^+$), 660 ($[Zn_3CuCp^*_3]^+$). IR: $\tilde{\nu}$ = 2936, 2878, 2832, 1407, 1371, 1250, 1175, 1082, 1032, 906, 881, 855, 791, 744 cm$^{-1}$.

The asymmetric unit of **1** contains two independent cations **A** and **B**; for clarity only one cation $[Zn_3Cp^*_3]^+$ is shown in Figure 2. Selected interatomic distances [Å] and angles [°] are given for both cations (**A**: Zn1,Zn2,Zn3; **B**: Zn4,Zn5,Zn6): Zn1–Zn2 2.430(1), Zn1–Zn3 2.418(1), Zn2–Zn3 2.463, Zn4–Zn5 2.432(1), Zn4–Zn6 2.432(1), Zn5–Zn6 2.407(1); Zn1-Zn2-Zn3 59.22(1), Zn1-Zn3-Zn2 59.71(1), Zn3-Zn1-Zn2 61.06(1), Zn6-Zn4-Zn5 59.47(1), Zn6-Zn5-Zn4 60.02(2), Zn5-Zn6-Zn4, 60.50(2). Calculated values at the M06L/TZVPP level: Zn–Zn 2.465; Zn-Zn-Zn 60.0. Selected interatomic distances [Å] and angles [°] for **2**: The calculated structural data at the M06L/TZVPP level are given in italics and Cp* denotes the centroid position: Zn1–Zn2 2.357(1) [*2.531*], Zn1–Cu1 2.381(1) [*2.355*], Zn2–Cu1 2.381(1) [*2.355*], Zn1–Cp* 1.883 [*1.906*], Zn2–Cp* 1.884 [*1.908*], Cu1–Cp* 1.893 [*1.809*]; Zn1-Zn2-Cu1 60.34(3) [*57.2*], Zn1-Cu1-Zn2 59.33(2) [*65.0*], Zn2-Zn1-Cu1 60.34(3) [*57.2*], M-M-Cp* 149.91 (average) (M = Zn, Cu) [*154.8*].

  

**Keywords:** aromaticity · clusters · copper · bonding analysis · density functional theory calculations · zinc

**How to cite:** *Angew. Chem. Int. Ed.* **2015**, *54*, 4370 – 4374
*Angew. Chem.* **2015**, *127*, 4445 – 4449

[1] T. Oka, *Proc. Natl. Acad. Sci. USA* **2006**, *103*, 12235 – 12242.
[2] J. O. Hirschfelder, *J. Chem. Phys.* **1938**, *6*, 795 – 806.
[3] A. N. Alexandrova, A. I. Boldyrev, *J. Phys. Chem. A* **2003**, *107*, 554 – 560.
[4] R. W. A. Havenith, F. De Proft, P. W. Fowler, P. Geerlings, *Chem. Phys. Lett.* **2005**, *407*, 391 – 396.
[5] a) T. J. Robilotto, J. Bacsa, T. G. Gray, J. P. Sadighi, *Angew. Chem. Int. Ed.* **2012**, *51*, 12077 – 12080; *Angew. Chem.* **2012**, *124*, 12243 – 12246.
[6] A. Mühlecker-Knoepfler, E. Ellmerer-Muller, R. Konrat, K.-H. Ongania, K. Wurst, P. Peringer, *J. Chem. Soc. Dalton Trans.* **1997**, 1607 – 1610.
[7] S. Blanchard, L. Fensterbank, G. Gontard, E. Lacôte, G. Maestri, M. Malacria, *Angew. Chem. Int. Ed.* **2014**, *53*, 1987 – 1991; *Angew. Chem.* **2014**, *126*, 2018 – 2022.
[8] X.-W. Li, W. T. Pennington, G. H. Robinson, *J. Am. Chem. Soc.* **1995**, *117*, 7578 – 7579.
[9] U. Mizutani, *Hume-Rothery Rules for Structurally Complex Alloy Phases*, CRC, Taylor & Francis, Boca Raton, FL, **2011**.
[10] a) T. Bollermann, K. Freitag, C. Gemel, M. Molon, R. W. Seidel, P. Jerabek, G. Frenking, R. A. Fischer, *Inorg. Chem.* **2011**, *50*, 10486 – 10492; b) T. Bollermann, K. Freitag, C. Gemel, R. W. Seidel, R. A. Fischer, *Organometallics* **2011**, *30*, 4123 – 4127; c) T. Bollermann, K. Freitag, C. Gemel, R. W. Seidel, M. von Hopffgarten, G. Frenking, R. A. Fischer, *Angew. Chem. Int. Ed.* **2011**, *50*, 772 – 776; *Angew. Chem.* **2011**, *123*, 798 – 802.
[11] T. Cadenbach, T. Bollermann, C. Gemel, I Fernandez, M. von Hopffgarten, G. Frenking, R. A. Fischer, *Angew. Chem. Int. Ed.* **2008**, *47*, 9150 – 9154; *Angew. Chem.* **2008**, *120*, 9290 – 9295.
[12] a) P. Pyykkö, N. Runeberg, *Angew. Chem. Int. Ed.* **2002**, *41*, 2174 – 2176; *Angew. Chem.* **2002**, *114*, 2278 – 2280; b) X. Wang, L. Andrews, I. Infante, L. Gagliardi, *J. Am. Chem. Soc.* **2008**, *130*, 1973-1978.
[13] a) G. J. Kubas, R. R. Ryan, B. I. Swanson, P. J. Vergamini, H. J. Wasserman, *J. Am. Chem. Soc.* **1984**, *106*, 451 – 452; b) G. J. Kubas, *Acc. Chem. Res.* **1988**, *21*, 120 – 128; c) G. J. Kubas, *Chem. Rev.* **2007**, *107*, 4152 – 4205.
[14] K. Freitag, H. Banh, C. Gemel, R. W. Seidel, S. Kahlal, J.-Y. Saillard, R. A. Fischer, *Chem. Commun.* **2014**, *50*, 8681 – 8684, and references in there.
[15] I. Resa, E. Carmona, E. Gutierrez-Puebla, A. Monge, *Science* **2004**, *305*, 1136 – 1138.
[16] a) M. A. Chilleck, T. Braun, B. Braun, *Chem. Eur. J.* **2011**, *17*, 12902 – 12905; b) K. Freitag, H. Banh, C. Ganesamoorthy, R. W. Seidel, C. Gemel, R. A. Fischer, *Dalton Trans.* **2013**, *42*, 10540 – 10544.
[17] Y. Zhao, D. G. Truhlar, *J. Chem. Phys.* **2006**, *125*, 194101.
[18] F. Weigend, R. Ahlrichs, *Phys. Chem. Chem. Phys.* **2005**, *7*, 3297.
[19] a) A. D. Becke, *Phys. Rev. A* **1988**, *38*, 3098; b) J. P. Perdew, *Phys. Rev. B* **1986**, *33*, 8822.
[20] S. Grimme, J. Antony, S. Ehrlich, H. Krieg, *J. Chem. Phys.* **2010**, *132*, 154104.
[21] P. Pyykkö, M. Atsumi, *Chem. Eur. J.* **2009**, *15*, 186 – 197.
[22] The calculations at BP86 with different basis sets without dispersion corrections gave nearly identical values for the Zn–Zn and Zn–Cu bonds which were, however, too long (2.56–2.59 Å).
[23] A. I. Boldyrev, L.-S. Wang, *Chem. Rev.* **2005**, *105*, 3716 – 3757.

Received: November 4, 2014
Revised: December 18, 2014
Published online: February 12, 2015

  